

ChemComm

Accepted Manuscript



This is an *Accepted Manuscript*, which has been through the Royal Society of Chemistry peer review process and has been accepted for publication.

Accepted Manuscripts are published online shortly after acceptance, before technical editing, formatting and proof reading. Using this free service, authors can make their results available to the community, in citable form, before we publish the edited article. We will replace this *Accepted Manuscript* with the edited and formatted *Advance Article* as soon as it is available.

You can find more information about *Accepted Manuscripts* in the [Information for Authors](#).

Please note that technical editing may introduce minor changes to the text and/or graphics, which may alter content. The journal's standard [Terms & Conditions](#) and the [Ethical guidelines](#) still apply. In no event shall the Royal Society of Chemistry be held responsible for any errors or omissions in this *Accepted Manuscript* or any consequences arising from the use of any information it contains.



ChemComm

COMMUNICATION

Near Infrared Light-driven Water Oxidation in a Molecule-based Artificial Photosynthetic Device Using an Upconversion Nano-photosensitizer

Received 00th January 20xx,
Accepted 00th January 20xx

DOI: 10.1039/x0xx00000x

www.rsc.org/

Xiaomin Liu,^{a†} Hung-Cheng Chen,^{b†} Xianggui Kong,^{*a} Youlin Zhang,^a Langping Tu,^a Yulei Chang,^a Fei Wu,^a Tongtong Wang,^a Joost N. H. Reek,^b Albert M. Brouwer,^{*b} Hong Zhang^{*ab}

We provide the first demonstration of a near infrared light driven water oxidation reaction in a molecule-based artificial photosynthetic device using an upconversion nano-photosensitizer. One very attractive advantage of this system is that using NIR light irradiation does not lead to significant photodamage, a serious problem in molecular based artificial photosynthesis under visible light irradiation.

Solar to fuel conversion by artificial photosynthetic devices has recently been considered as a promising approach to produce sustainable energy.^{1,2} One of the options is solar driven water splitting by photoelectrochemical cells, resulting in the production of O₂ and H₂, which can be used as a clean fuel.³ The process consists of two half reactions: a proton reduction reaction at the photocathode and a water oxidation at the photoanode. Of these two half reactions, water oxidation is the more challenging process because it involves an endergonic four-electron process and therefore it often requires a large overpotential.⁴ In photoanode design for photocatalytic water oxidation, effective catalyst and photoactive dye-sensitizer with broad-band light-harvesting function are needed to make this reaction as efficient as possible.⁵ Recently, we have successfully developed a novel photosensitizer Pt(II)-porphyrin (Pt(II)-TCPP) with a high potential of the radical cation/neutral redox couple that provides a driving force for favorable electron transfer between the catalyst and photo-oxidized Pt(II)-TCPP.⁶ Moreover, the photon capture ability is about three times higher than that of the widely used photosensitizer tris (2,2'-bipyridyl) ruthenium(II), [Ru(bpy)₃]²⁺. Pt(II)-TCPP can utilize ultraviolet ~ visible light < 555 nm for water-splitting when it is properly coupled to an active water oxidation catalyst. In order to further improve the photon capture ability and potentially increase the solar to fuel conversion efficiency, the general design strategy is to introduce a cascade of events including excitation energy

transfer by an artificial antenna with a multi-chromophore system.⁷⁻⁹ However, the bottleneck of solar driven water oxidation efficiency is still the limited absorption spectral range of the photosensitizer. The solution is to extend the absorption of the artificial photosynthetic system to longer wavelengths. In particular, the near-infrared (NIR) region contains ~ 40 % solar flux which usually remains unused.¹⁰

It is known that the light-harvesting units in photosystem II play a photo-protection role for avoiding photodamage by the safe thermal dissipation energy mechanisms under excess light.¹¹⁻¹⁴ Likewise, improving photostability is always a big concern in artificial photosynthetic device development for long-term activity.⁵ Although several mimicking models with photo-protection function have been proposed, there is still a formidable challenge for further improving photocatalytic water oxidation.¹⁵⁻¹⁷ The advent of nanotechnology allows to integrate several photocatalytic elements in a nanoplatform^{18,19} and can also lead to new approaches to minimizing the photodamage effect.

Herein, we constructed NaYF₄:Yb³⁺,Er³⁺ upconversion nanoparticles (UCNPs) covalently conjugated with our recently developed Pt(II)-TCPP photosensitizers. This nano-photosensitizer (UCNPs/Pt(II)-TCPP) can be excited with NIR light (~ 920 - 980 nm) and utilizes the NIR photons to bring the Pt(II)-TCPP photosensitizer in its excited state. This is capable to drive photocatalytic water oxidation coupled to a Co₄O₄-cubane complex as water-oxidation catalyst in neutral phosphate buffer solution (Figure 1b).⁶ Furthermore, our nano-photosensitizer for NIR light driven water oxidation provides a novel design to prevent photodamage. For investigating the NIR-driven photocatalytic water oxidation activity, the conventional three component systems composed of nano-photosensitizer, sacrificial electron acceptor and water oxidation catalyst were employed.

Hydrophobic NaYF₄: 20% Yb³⁺, 0.2% Er³⁺ UCNPs were used as the energy donor. They are in hexagonal phase and possess uniform morphology with average diameter about 26±2 nm (Fig. S1a and S2). The hydrophilic NH₂-functionalized UCNPs were then prepared via a ligand exchange process using poly(allylamine) as surface coating agent. To ensure that the majority of Pt(II)-TCPP molecules were firmly linked to UCNPs, a covalent conjugation strategy was followed that involved a cross-linking reaction between the amino group of the UCNPs and the carboxyl group of the Pt(II)-TCPP, see Fig. 1a. Changes in the sizes of the nanoparticles before and after

^a State Key Laboratory of Luminescence and Applications, Changchun Institute of Optics, Fine Mechanics and Physics, Chinese Academy of Sciences, Changchun 130033 (P. R. China)

^b Van't Hoff Institute for Molecular Sciences, University of Amsterdam, Science Park 904, 1098 XH Amsterdam

[†] These authors contributed equally

Electronic Supplementary Information (ESI) available: [Experimental section and additional data.]. See DOI: 10.1039/x0xx00000x

conjugation with Pt(II)-TCPP could not be deduced from the TEM images (Fig. S1a and S1b) since the polymer coating are not readily observable in TEM images. In order to directly visualize the polymer shell, the sample was stained with phosphotungstic acid, which increases the contrast and makes the shells appear as halos surrounding the nanoparticles (Fig. S1c). The polymer shell thickness was thus measured to be about 4.5 nm (Fig. S1d). Coupling of the UCNP with Pt(II)-TCPP was also confirmed by FTIR absorption spectra (Fig. S3). The change in the carbonyl region (1650 - 1710 cm^{-1}) indicates bond formation between the carboxylic acid group of Pt(II)-TCPP and the amino group of the nanoparticles. The loading capacity of Pt(II)-TCPP was then studied. Fig. S4 shows that the absorption intensities increased with the amount of added Pt(II)-TCPP, and saturated at 13%(w/w). Owing to the robust covalent bonding between Pt(II)-TCPP and $\text{NaYF}_4:\text{Yb}^{3+}, \text{Er}^{3+}$, we could bind at most ~ 2200 Pt(II)-TCPP molecules to each UCNP.

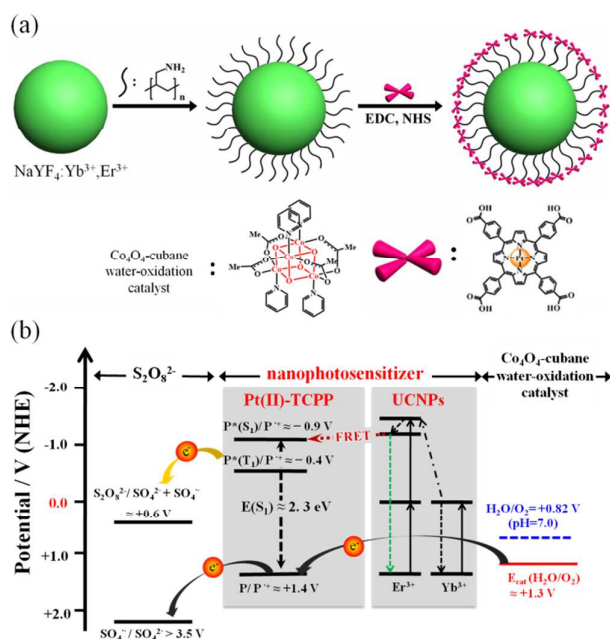


Fig. 1 (a) Construction of the $\text{NaYF}_4:\text{Yb}^{3+}, \text{Er}^{3+}$ UCNP/Pt(II)-TCPP nano-photosensitizer. (b) Energy scheme of UCNP/Pt(II)-TCPP and water oxidation catalyst.

The design of this nano-photosensitizer is based on energy transfer from upconversion luminescent (UCL) states of UCNP to photosensitizers. Effective energy transfer can be achieved by properly choosing a photosensitizer of which the absorption matches a desired UCL band of UCNP and by shortening the interaction distance between the energy donor and acceptor.²¹⁻²³ Hybrid upconversion nano-photosensitizers have been successfully applied in different fields.²⁴⁻²⁶ Recently, improved solar water-splitting efficiency in semiconductor photoelectrode film incorporating UCNP was also reported.^{27,28} In the present study, a photosensitizing molecule, Pt(II)-TCPP, was chosen because its absorption spectrum overlaps with the green UCL band (520 - 570 nm) (see Fig. 2a). Fig. 1(b) depicts the energy level scheme for photocatalytic components and reaction procedures. Firstly, under the excitation of 980 nm, the excited state Pt(II)-TCPP molecules are prepared via energy transfer from the green emission band of

UCNP. Subsequent highly exothermic triplet-state one-electron transfer reaction from photogenerated $^3\text{Pt(II)-TCPP}$ to $\text{S}_2\text{O}_8^{2-}$ in buffer solution results in formation of the Pt(III)-porphyrin radical cation. This species with high reduction potential is thermodynamically capable to drive WOCs to oxidize water to O_2 . The energy transfer from UCNP to Pt(II)-TCPP was confirmed from both steady-state UCL spectra and UCL decay kinetics. The UCL spectra of Fig. 2b demonstrate that under excitation at 980 nm, the 540 nm band was strongly quenched by Pt(II)-TCPP, while the 650 nm band remained unchanged. The energy transfer efficiency can be estimated from the quenching of UCL emission: $E = (I_0 - I_1) / I_0$, where I_0 and I_1 are green emission intensities of UCNP before and after conjugation with Pt(II)-TCPP, respectively. From this formula, the energy transfer efficiency of the 540 nm band was determined as high as 96.3% for the present covalently bonded nanoconjugates.

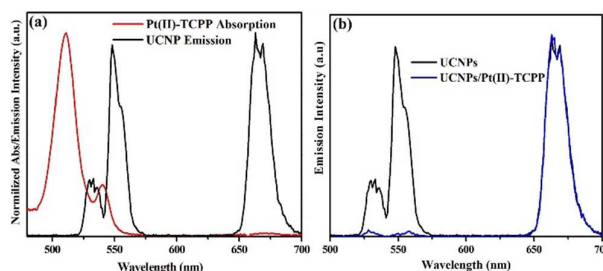


Fig. 2 (a) Spectral overlap between the emission of the donor UCNP and the absorption of the acceptor Pt(II)-TCPP in pH=7.0, 0.1M phosphate buffer. (b) Emission spectra of NH_2 -functionalized UCNP and UCNP/Pt(II)-TCPP nano-photosensitizer under excitation at 980 nm (normalized by the intensity at 650 nm).

The dynamic energy transfer process, i.e. Förster resonant energy transfer (FRET), was studied by the temporal behavior of UCL recorded at 540 nm and 650 nm (Fig. S5). In the presence of Pt(II)-TCPP, the average decay time decreases from $\sim 150 \mu\text{s}$ to $\sim 80 \mu\text{s}$ for 540 nm (Fig. S5a), whereas the average decay time at 650 nm shows hardly any change due to the poor absorption of Pt(II)-TCPP in this region (Fig. S5b). The dynamic energy transfer efficiency, calculated as $(\tau_0 - \tau_1) / \tau_0$, shows a value of 46.7% at 540 nm, which is less than the value determined from the steady-state UCL spectra (96.3%). This discrepancy indicates that re-absorption of Pt(II)-TCPP that is radiative and static in nature is non-negligible in the energy transfer process, i.e. both radiative and nonradiative energy transfer coexist in this case. However, the radiative energy transfer process does not alter the temporal behavior of UCL. For comparison we have also setup a model of radiative energy transfer by mixing UCNP and Pt(II)-TCPP. The decay time at 540 nm shows almost no change (Fig. S5c). In other words, the efficient energy transfer from UCNP to Pt(II)-TCPP in the nano-photosensitizer ensures an effective photogeneration of excited Pt(II)-TCPP under NIR excitation.

Photocatalytic water oxidation experiments were carried out in solutions containing 1.83×10^{-3} M UCNP/Pt(II)-TCPP nano-photosensitizer as evaluated by Pt(II)-TCPP absorption, 0.15 M $\text{Na}_2\text{S}_2\text{O}_8$ and 1.5×10^{-4} M catalysts Co_4O_4 -cubane in phosphate buffer solution (0.1 M, pH = 7.0) at room temperature. Photocatalytic oxygen generation was monitored through the detection of dissolved O_2 using a Clark-type electrode. A 980 nm continuous diode laser was used as the irradiation source. The result of light driven oxygen formation is shown in Fig. 3a. Control

experiments were carried out in which each individual component of the system was removed. Significant oxygen generation was only observed when all three components were present (Fig. S6). A comparison was made between the covalently conjugated UCNP/Pt(II)-TCPP nano-photosensitizer and the mixture as indicated in Fig. 3a. The maximum turnover frequency TOF_{max} of the catalyst was observed to be $6.6 \times 10^{-4} \text{ mol O}_2 (\text{mol of Co}_4\text{O}_4\text{-cubane})^{-1}\text{s}^{-1}$ in the nano-photosensitizer (excitation power 750 mW). However, the TOF_{max} was reduced to $9.6 \times 10^{-5} \text{ mol O}_2 (\text{mol of Co}_4\text{O}_4\text{-cubane})^{-1}\text{s}^{-1}$ in the mixture of UCNPs and Pt(II)-TCPP. These results indicate that efficient energy transfer in the covalently conjugated nano-photosensitizer improves significantly the light driven water oxidation activity, compared to the re-absorption process only in the mixture of UCNPs and Pt(II)-TCPP under the same excitation condition. A further control experiment was conducted using Pt(II)-TCPP as the unique photosensitizer. Because Pt(II)-TCPP did not show any electronic absorption in NIR range, there was, as expected, no oxygen evolution under the excitation of 980 nm light.

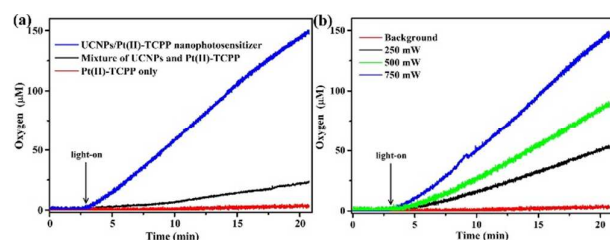


Fig. 3 (a) Photochemical oxygen evolution in 1.5 mL of a pH 7.0, 0.1M phosphate buffer solution containing Co_4O_4 cubane (1.5×10^{-4} M), $\text{Na}_2\text{S}_2\text{O}_8$ (0.15 M) and UCNP/Pt(II)-TCPP nano-photosensitizer (1.83×10^{-3} M) (blue line); a mixture of UCNPs and Pt(II)-TCPP (black line). The red line is the control experiment with Pt(II)-TCPP only. Excitation was at 980 nm (750 mW). (b) Photochemical oxygen evolution with various excitation powers (980nm laser) in 1.5 mL of a pH 7.0, 0.1M phosphate buffer solution containing $\text{Na}_2\text{S}_2\text{O}_8$ (0.15 M), UCNP/Pt(II)-TCPP (1.83×10^{-3} M) and catalyst Co_4O_4 cubane (1.5×10^{-4} M).

In order to investigate whether the TOF values are limited by the photon absorption rate or the inherent catalytic activity of the WOC, the light driven water oxidation activities were measured at different excitation powers (250 mW, 500 mW and 750 mW) of incident 980 nm laser light. The results are shown in Fig. 3b. The obtained values of TOF_{max} are 2.4×10^{-4} , 4.1×10^{-4} and $6.6 \times 10^{-4} \text{ mol O}_2 (\text{mol of Co}_4\text{O}_4\text{-cubane})^{-1}\text{s}^{-1}$ under 250 mW, 500 mW and 750 mW, respectively, i.e. TOF increases with increasing excitation power. This result shows that NIR indirect excitation of Pt(II)-TCPP can keep up with the catalytic water oxidation cycle in this excitation power range. The overall quantum yield of NIR photons induced O_2 generations is $\sim 9 \times 10^{-3} \%$ in UCNP/PtTCPP nanophotosensitizer under excitation with three different powers of 980 nm NIR-laser (details of the calculation see S1).

Photostability is a major concern for the performance of photosensitizers for photocatalytic water oxidation. UCNP, which act as nanotransducer to convert NIR light to visible wavelengths, afford an indirect, but local, light source which ensures that the excitation NIR light does not interact with any organic molecules in solution until it encounters the UCNP/Pt(II)-TCPP nano-photosensitizer, different from the scenario directly using visible

light irradiation. The photon energy can be effectively utilized since the surface of each UCNP is anchored with plenty of photosensitizers to accept the upconverted energy from the UCNP, and thus can effectively avoid photodamage and greatly prolong the service life of the device. As shown in Fig. 4, 1.5 mL of a pH 7.0, 0.1 M phosphate buffer solution containing $\text{Na}_2\text{S}_2\text{O}_8$ (0.15 M), UCNP/Pt(III)-TCPP (1.83×10^{-3} M) and Co_4O_4 -cubane (1.5×10^{-4} M) was irradiated under 980 nm laser (indirect irradiation) and 532 nm laser (direct irradiation) for comparison. The power of the laser was 300 mW for 980 nm and 100 mW for 532 nm, respectively, which led to almost equal oxygen generation rates (Fig. 4a). After irradiation for 20 min, UV-Vis absorption spectra were recorded to evaluate the photostability, as shown in Fig. 4b. The UV-Vis absorption spectrum of the sample after 980 nm irradiation did not show any change. In contrast, the UV-Vis absorption spectrum of the sample was completely changed upon 532 nm irradiation, indicating severe photodamage under direct excitation. The photos of the samples before and after light irradiation of the two different wavelengths (inset in Fig. 4b and Fig. S7) provide a vivid illustration of the difference in photostability under different conditions.

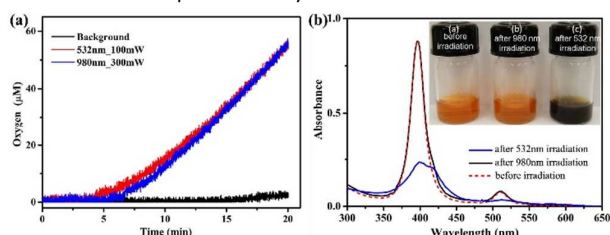


Fig. 4 (a) Photochemical oxygen evolution in 1.5 mL of a pH 7.0, 0.1 M phosphate buffer solution with different excitation powers of 980 nm laser (300 mW, blue) and 532 nm green laser (100 mW, red). (b) Absorption spectra of samples before irradiation, after 980 nm irradiation and after 532 nm irradiation. The insert in the figure shows the photos of the samples before and after irradiations.

To understand this phenomenon we need to go into the working mechanism of the photosynthetic device. The energy level diagram is shown in Fig. 1b including combinations of water oxidation catalyst, nano-photosensitizer and sacrificial electron acceptor ($\text{Na}_2\text{S}_2\text{O}_8$) in neutral phosphate buffer. Under the excitation of 980 nm, Pt(III)-TCPP molecules are prepared in the excited state via energy transfer from UCNP. Highly exothermic electron transfer from photogenerated $^3\text{Pt(II)-TCPP}$ to $\text{S}_2\text{O}_8^{2-}$ in buffer solution results in formation of Pt(II)-porphyrin radical cation. This species is thermodynamically capable to drive the water oxidation catalyst to oxidize water to O_2 .⁶ The UCNP/Pt(II)-TCPP nano-photosensitizer solution without addition of sacrificial electron acceptor (sodium persulfate) retains similar absorption spectra under light irradiation of both excitation wavelengths (see Fig. S8). This indicates that the photodamage paths are mostly related to the radical cation of Pt(II)-TCPP. The reduction of the radical cation of the photosensitizer by the water oxidation catalyst is rate limiting in general.²⁹ Therefore side reactions of the radical cation may be relatively enhanced at high incident light power. Because the porphyrin radical cation in water shows a broad and intense absorption in the UV-visible range and has a lifetime that can be up to seconds.^{30,31} Visible light (e.g. 532 nm) may cause photochemical degradation via the excited state of the metalloporphyrin radical cation. Conversely, photo-absorption of porphyrin radical cation can be excluded at 980 nm. Since most of the upconverted 540 nm

band contributes to bringing the photosensitizers to the excited states due to the efficient energy transfer between the UCNP and photosensitizers, the residual upconverted 540 nm band is much weaker than the direct 532 nm laser irradiation for the photodamage of the radical cations, which might be responsible for the significantly enhanced photostability of UCNP/Pt(II)-TCPP nano-photosensitizer under NIR excitation.

In conclusion, we have demonstrated a novel NIR driven nano-photosensitizer, integrating UCNP with Pt(II)-TCPP. The excited state of this sensitizer has sufficient oxidizing power to drive the water splitting reaction when an appropriate catalyst is present. To the best of our knowledge, this is the first demonstration of a light driven water oxidation reaction using only near-infrared photons in a molecule-based artificial photosynthetic device. Furthermore, the UCNP/Pt(II)-TCPP nano-photosensitizer also significantly improves the photostability of the solution under NIR light excitation compared to the scenario of visible light excitation. The upconversion efficiency should be further improved for practical applications in actual solar driven catalysis. This can be achieved by manipulating emission and excitation processes through structure design or plasmonic coupling.^{32,33} Consequently, harvesting NIR photons for light driven water oxidation by artificial photosynthesis can be achieved under solar irradiation.

Notes and references

- S. Bensaid, G. Centi, E. Garrone, S. Perathoner and G. Saracco, *ChemSusChem*. 2012, **5**, 500.
- T. R. Cook, D. K. Dogutan, S. Y. Reece, Y. Surendranath, T. S. Teets and D. G. Nocera, *Chem. Rev.* 2010, **110**, 6474.
- M. G. Walter, E. L. Warren, J. R. McKone, S. W. Boettcher, Q. Mi, E. A. Santori and N. S. Lewis, *Chem. Rev.* 2010, **110**, 6446.
- H. Dau, C. Limberg, T. Reier, M. Risch, S. Roggan and P. Strasser, *ChemCatChem*. 2010, **2**, 724.
- J. R. Swierk and T. E. Mallouk, *Chem. Soc. Rev.* 2013, **42**, 2357.
- H. C. Chen, G. H. Hettterscheid, R. M. Williams, J. I. Van der Vlugt, J. N. H. Reek and A. M. Brouwer, *Energy Environ. Sci.* 2015, **8**, 975.
- H. J. Imahori, *Phys. Chem. B*. 2004, **108**, 6130.
- D. Gust, T. A. Moore and A. L. Moore, *Acc. Chem. Res.* 2009, **42**, 1890.
- F. Puntoriero, G. Ganga, A. Sartorel, M. Carraro, G. Scorrano, M. Bonchio, S. Campagna, *Chem. Commun.* 2010, **46**, 4725.
- N. D. McDaniel S. Bernhard, *Dalt. Trans.* 2010, **39**, 10021.
- J. Barber, B. Andersson, *Trends Biochem Sci.* 1992, **17**, 61.
- H. A. Frank, G. W. Brudvig, *Biochemistry* 2004, **43**, 8607.
- N. E. Holt, G. R. Fleming, K. K. Niyogi, *Biochemistry*. 2004, **43**, 8281.
- G. Scholes, G. Fleming, A. Olaya-Castro and R. Van Grondelle, *Nat. Chem.* 2011, **3**, 763.
- R. Berera, C. Herrero, I. H. M. Van Stokkum, M. Vengris, G. Kodis, R. E. Palacios, H. Van Amerongen, R. Van Grondelle, D. Gust and T. A. Moore, *Proc. Natl. Acad. Sci. U. S. A.* 2006, **103**, 5343.
- S. D. Straight, G. Kodis, Y. Terazono, M. Hambourger, T. A. Moore, A. L. Moore, D. Gust, *Nat. Nanotechnol.* 2008, **3**, 280.
- Y. Terazono, G. Kodis, K. Bhushan, J. Zaks, C. Madden, A. L. Moore, G. R. Fleming and D. Gust, *J. Am. Chem. Soc.* 2011, **133**, 2916.
- G. Yuan, A. Agiral, N. Pellet, W. Kim and H. Frei, *Faraday Discuss.* 2014, **176**, 233.
- T. Itoh, K. Yano, T. Kajino, S. Itoh, Y. Shibata, H. Mino, R. Miyamoto, Y. Inada, S. Iwai and Y. Fukushima, *J. Phys. Chem. B*. 2004, **108**, 13683.
- L. Duan, L. Tong, Y. Xu, L. Sun, *Energy Environ. Sci.* 2011, **4**, 3296.
- G. Chen, H. Qiu, P. N. Prasad and X. Chen, *Chem. Rev.* 2014, **114**, 5161.
- X. Han, R. Deng, X. Xie, X. Liu, *Angew. Chem. Int. Ed.* 2014, **53**, 11702.
- J. Liu, Y. Liu, Q. Liu, C. Li, L. Sun, F. Li, *J. Am. Chem. Soc.* 2011, **133**, 15276.
- T. Q. Wu, J. C. Boyer, M. Barker, D. Wilson, N. R. Branda, *Chem. Mater.* 2013, **25**, 2495.
- X. Lu, X. G. Kong, X. M. Liu, L. P. Tu, Y. L. Zhang, Y. L. Chang, K. Liu, D. Z. Shen, H. Y. Zhao and H. Zhang, *Biomaterials*. 2014, **35**, 4146.
- N. M. Idris, M. K. Gnanasammandhan, J. Zhang, P. C. Ho, R. Mahendran, Y. Zhang, *Nat Med* 2012, **18**, 1580.
- M. Zhang, Y. Lin, T. J. Mullen, W. F. Lin, L. D. Sun, C. H. Yan, T. E. Patten, D. Wang, G. Y. Liu, *J. Phys. Chem. Lett.* 2012, **3**, 3188.
- F. Gonell, M. Haro, R. S. Sa, P. Negro, B. Julia, *J. Phys. Chem. C* 2014, **118**, 11279.
- W. J. Youngblood, S. H. A. Lee, Y. Kobayashi, E. A. Hernandez-Pagan, P. G. Hoertz, T. A. Moore, A. L. Moore, D. Gust and T. E. Mallouk, *J. Am. Chem. Soc.* 2009, **131**, 926.
- A. Harriman, P. Neta and M. C. Richoux, *J. Phys. Chem.* 1986, **90**, 3444.
- A. Harriman, G. Porter, P. Walters, *J. Chem. Soc. Faraday Trans.* 1983, **79**, 1335.
- W. Zou, C. Visser, J. A. Maduro, M. S. Pshenichnikov and J. C. Hummelen, *Nat. Photonics* 2012, **6**, 560.
- D. M. Wu, A. Garcia-Etxarri, A. Salleo, J. A. Dionne, *J. Phys. Chem. Lett.* 2014, **5**, 4020.